

Improvement of flux and torque ripple in direct torque control (DTC) of induction motor using improved switching tables

Rahmat Aazami ^{1,*}, Saman Esmailbeigi ² and Mohammadamin Shirkhani ¹

¹ Department of Electrical Engineering, Ilam University, Ilam, Iran

² Department of Electrical Engineering, Shahid Beheshti University, Tehran, Iran

E-mail addresses: r.aazami@ilam.ac.ir ; ma.shirkhani@ilam.ac.ir ; samanesmaeilbeygi@gmail.com

*Corresponding author

Received: 02/11/2023, Revised: 21/11/2023, Accepted: 28/11/2023.

Abstract

Direct Torque Control (DTC) is one of the novel methods of the induction motor control in which the torque generated by the induction motor is controlled directly by the inverter switching modes. The direct torque control method has advantages than other induction motor control methods, which include: 1- Non-use of current controllers 2- Remove rotor positioning sensors 3- Quick torque response 4- Lack of dependence on some parameters of the induction motor and 5- lack of need to control any axis of the motor. Due to these features, this method has become one of the popular methods of the induction motor control in industry. But it still has some disadvantages, such as a high ripple in the curves of electromagnetic torque and stator flux, as well as the inappropriate performance at low engine speeds. In this paper, various strategies for direct torque control of the induction motor have been investigated and an improved switching table has been proposed as well as a switching table with 12 regions that are compared with other methods and results indicate that the direct torque control strategy using 12 regions, improves the flux and torque ripple to a satisfactory level. The simulation was performed in Simulink/ Matlab and the results are presented in the simulation section.

Keywords

Direct Torque Control (DTC), Squirrel cage induction motor control, flux and torque ripp, Induction Motor, Switching Table.

1. Introduction

At first, the speed control of electrical machines was driven by direct current machines traditionally, since the magnetic flux and electromagnetic torque are in direct relationship with the stator current and the rotor respectively. In the past 20 years, direct current machines (DC) have given way to induction machines and their abundant application is undeniable in the industry. However, due to their coupled nonlinear structure, the coupling between stator and rotor windings varies over time, which makes it is difficult to control this type of motor. The vector control method (FOC) has been used in the industry for many years and instead of direct current motors, AC machines with this type of control was used. The vector control method (FOC) is similar to the DC motor control which has a fast torque response but for optimal performance, it needs to specify motor parameters accurately and the dependence of this method on the induction motor parameters is one of its disadvantages [1-6].

In the last two decades, in order to improve the performance of the induction motor, a new direct torque control (DTC) of induction motor method was proposed by Japanese and German researchers. This method acts on the basis of selecting the most suitable voltage vector to maintain the curve of electromagnetic flux and torque

in the bandwidth defined in the hysteresis controllers of flux and torque[7, 8]. A lot of research has been done to improve the DTC in recent years. In[9, 10], a direct torque control method is proposed based on which the stator flux curve is directed at a specified path and by inverter switching frequency reduction by the specified reference value for it. In[11, 12], a control scheme based on direct torque control has proposed in which the rotor reference flux has used instead of the stator reference flux. In this method, the use of rotor and stator flux control have combined without knowing the position of the rotor flux. This idea requires the use of induction motor parameters that has usually encountered with saturation problems. In the common DTC method, two hysteresis controllers for flux and torque are used in which flux hysteresis controller is two-levels and torque hysteresis controller is three-levels. The bandwidth of the hysteresis controllers has a great influence on the stator current curve. So that, by decreasing the bandwidth of the hysteresis controllers, the stator current curve approaches a sinusoidal wave [13]. In [14]different methods of artificial intelligence have been investigated on direct torque control, In the case of using fuzzy logic, neural networks as and hybrid fuzzy logic, the flux, and torque ripple decrease significantly.

In this paper, first introduces the common direct torque control (DTC) scheme and then compares it with other methods based on direct torque control. Various articles have been done in this field [15-17], but the methods presented in this article have good performance in terms of torque ripple and flux ripple. Due to the adjustment of the parameters controlling the hysteresis flux and torque in all three conventional methods, it has improved and the 12 ripple flux regions, especially the torque ripple, have had an acceptable reduction compared to the normal state. Also in some similar papers, a synchronous motor as well as a dual feed induction generator have been used to test the work, but in this paper the squirrel cage induction motor has been used. The results show that by applying this type of proposed switching table, the stator flux ripple and electromagnetic torque will be reduced to an acceptable level and the problems that were in the common DTC, somewhat resolved.

2. General DTC Structure

The DTC method includes different parts such as switching tables, flux and torque hysteresis controllers, speed estimator, voltage source inverter, PID controller and several other components. In this method, the voltage and current of a motor are sampled and, based on the voltage and current values sampled, the amount of stator flux is calculated. Then, using the current and flux values, the electromagnetic torque is calculated. The values of flux and torque are compared with their reference values and are given to hysteresis controllers, the outputs of these controllers are used for inverter switching. An overview of the DTC method is given in figure 1.

The state space voltage of the three-phase inverter, which is the induction motor stator windings input, is given in equation 1:

$$v_{sn} = \frac{2}{3} v_{dc} e^{\frac{j(n-1)\pi}{3}} \text{ for } \dots 1, 2, 3, 4, 5, 6$$

$$0 \text{ for } \dots 0, 7 \quad (1)$$

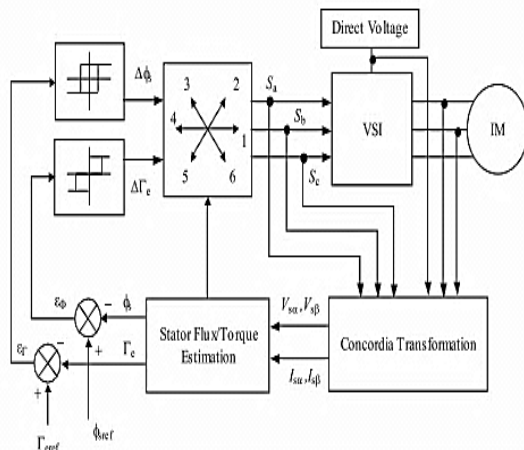


Fig. 1. An overview of the DTC method.

In which the variable n specifies different areas for inverter operation. Voltage vectors for the six regions are shown in Figure 2. Indirect torque control, spatial vectors are used, for this reason, the real and imaginary parts of the stator voltage converted from the three-axis device

into a two-axis device using the following transformation [18].

$$\begin{bmatrix} v_{sa} \\ v_{sb} \\ v_{sc} \end{bmatrix} = \frac{2}{3} \begin{bmatrix} \cos \theta & \cos(\theta - \frac{2\pi}{3}) & \cos(\theta + \frac{2\pi}{3}) \\ \sin \theta & \sin(\theta - \frac{2\pi}{3}) & \sin(\theta + \frac{2\pi}{3}) \\ \frac{1}{2} & \frac{1}{2} & \frac{1}{2} \end{bmatrix} \begin{bmatrix} v_a \\ v_b \\ v_c \end{bmatrix} \quad (2)$$

2.1. Calculation of Stator Flux

The stator flux vector is calculated using the stator voltage vector and the stator winding resistance:

$$\phi_s = \frac{1}{T_N} \int_0^t (V_s - R_s I_s) dt + \phi_{s0} \quad (3)$$

In equation (3), ϕ_{s0} is the value of the flux linkage at the instant $t = 0$.

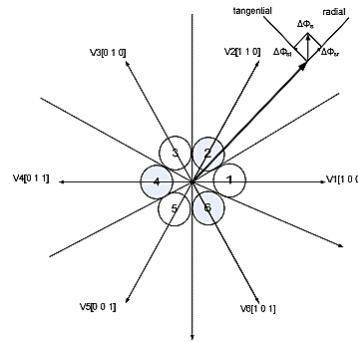


Fig. 2. Output voltage vectors of inverter and stator flux vector with six regions.

If the stator resistance is ignored, the stator flux variations are obtained by the following equation:

$$\Delta \phi_s = V_s \Delta t \quad (4)$$

In which $\Delta \phi_s$ represents the variations rate of the stator flux which has been created by a new voltage vector. This equation shows that the variations in the stator flux depend on the input voltage vector applied during the time interval Δt . Fig. 2 shows the stator flux vector, which contains the radial component $\Delta \phi_{sr}$ and the tangential component of $\Delta \phi_{st}$ [19, 20], and shows that if the stator flux increases, we must select a voltage vector that generates a greater radial component of the stator flux.

2.2. Calculation of Electromagnetic Torque

The electromagnetic torque is obtained in induction motors using Equation (5) [13, 21]:

$$T_e = P \frac{L_m}{\sigma L_s L_r} |\phi_s| * |\phi_r| * \sin \theta_{sr} \quad (5)$$

In the high equation, P the number of machine poles, L_m the stator and rotor mutual-inductance, L_s the stator self-inductance and the L_r are the self-inductance of the rotor windings. In steady state, the stator and rotor flux sizes are almost constant and so, the electromagnetic torque depends on the angle between the stator and rotor flux vector (θ_{sr}). So that by increasing the angular value between the stator and rotor flux vector, The electromagnetic torque increases and vice versa.

2.3. Hysteresis Controllers of Torque and Flux

Hysteresis controllers' performance are shown in figure 3 and 4. The torque and stator flux are estimated using equations 6 and 7:

$$T_e = \frac{3}{2} P [\phi_{s\alpha} I_{s\beta} - \phi_{s\beta} I_{s\alpha}]$$

(6)

$$\phi_s = \sqrt{(\phi_{s\alpha}^2 + \phi_{s\beta}^2)} \tag{7}$$

Estimated values are compared with their reference values, and the resulting error value is given to hysteresis controllers of flux and torque. The output of the hysteresis controllers produces an integer that indicates the increase or decrease in each of the flux and torque values.

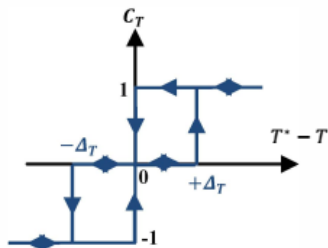


Fig.3. Hysteresis controller of torque [1]

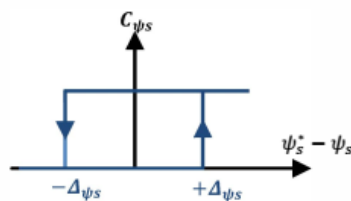


Fig.4. Hysteresis controller of flux [1]

Then the position of the stator flux vector is calculated by Eq. (8):

$$\theta_s = \tan^{-1} \left(\frac{\phi_{s\beta}}{\phi_{s\alpha}} \right) \tag{8}$$

Using the switching table 1, suitable voltage vectors are selected for switching the voltage source inverter (VSI). The applied voltage vectors will affect each of the electromagnetic flux and torque. So that if the flux vector is in region i , the voltage vectors of V_{i+1} or V_{i-1} will increase the flux amplitude and the V_{i+2} or V_{i-2} vectors will decrease the amplitude. Similarly, the voltage vectors of the V_{i+1} and V_{i+2} will increase the torque, and the V_{i-1} and V_{i-2} vectors will reduce the amount of torque produced by the motor.

Table1. General DTC switching table

Outputs of hysteresis controllers		sector					
C_{ψ_s}	C_{T_e}	1	2	3	4	5	6
1	1	V_2	V_3	V_4	V_5	V_6	V_1
	0	V_7	V_0	V_7	V_0	V_7	V_0
	-1	V_6	V_1	V_2	V_3	V_4	V_5
0	1	V_3	V_4	V_5	V_6	V_1	V_2
	0	V_0	V_7	V_0	V_7	V_0	V_7
	-1	V_5	V_6	V_1	V_2	V_3	V_4

Table2. Switching table of improved scheme

Outputs of hysteresis controllers		sector					
C_{ψ_s}	C_{T_e}	1	2	3	4	5	6
1	1	V_2	V_3	V_4	V_5	V_6	V_1
	0	V_7	V_0	V_7	V_0	V_7	V_0
	-1	V_1	V_2	V_3	V_4	V_5	V_6
0	1	V_4	V_5	V_6	V_1	V_2	V_3
	0	V_7	V_0	V_7	V_0	V_7	V_0
	-1	V_5	V_6	V_1	V_2	V_3	V_4

3. Direct torque control using improved switching tables and 6 regions

A We found that in the general DTC, the first region of the six regions was bound from the angle of -30 degrees to +30 degrees, but in the improved switching table (table 2), the first region is bounded from zero to

+60 degrees; in other words, the six regions have 30 degrees of angle variation (figure.5)[1]. The improved switching table is obtained by changing the 30 degrees of region. The improved switching table is presented in table 2.

Table3: Flux and torque variations due to the use of different voltage vectors

Applied voltage vector	General DTC (-30 and +30)	Improved DTC (0 and 60)
V1	Ambiguity in torque	Flux increases and torque increase
V2	Torque increase and flux increase	Torque increase and flux decrease
V3	Torque increase and flux decrease	Ambiguity in flux
V4	Ambiguity in torque	Torque increase and flux decrease
V5	Torque decreases and flux decrease	Torque decreases and flux decrease
V6	Torque decreases and flux increase	Ambiguity in flux

Table4. DTC switching Table in 12-Region Method

Outputs of hysteresis controllers		sector											
$C_{\phi s}$	C_{T_e}	1	2	3	4	5	6	7	8	9	10	11	12
1	2	V ₂	V ₃	V ₃	V ₄	V ₄	V ₅	V ₅	V ₆	V ₆	V ₁	V ₁	V ₂
	1	V ₂	V ₂	V ₃	V ₃	V ₄	V ₄	V ₅	V ₅	V ₆	V ₆	V ₁	V ₁
	-1	V ₁	V ₁	V ₂	V ₂	V ₃	V ₃	V ₄	V ₄	V ₅	V ₅	V ₆	V ₆
	-2	V ₆	V ₁	V ₁	V ₂	V ₂	V ₃	V ₃	V ₄	V ₄	V ₅	V ₅	V ₆
0	2	V ₃	V ₄	V ₄	V ₅	V ₅	V ₆	V ₆	V ₁	V ₁	V ₂	V ₂	V ₃
	1	V ₄	V ₄	V ₅	V ₅	V ₆	V ₆	V ₁	V ₁	V ₂	V ₂	V ₃	V ₃
	-1	V ₇	V ₅	V ₀	V ₆	V ₇	V ₁	V ₀	V ₂	V ₇	V ₃	V ₀	V ₄
	-2	V ₅	V ₆	V ₆	V ₁	V ₁	V ₂	V ₂	V ₃	V ₃	V ₄	V ₄	V ₅

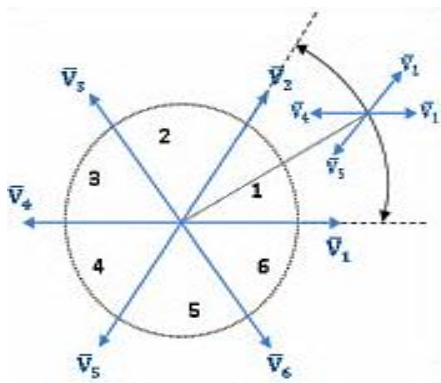


Fig.5. The six regions of the improved scheme.

According to Table 3 in the general DTC, two voltage vectors V1 and V4 have not been used because this voltage vector, depending on the location of the stator flux vector, can increase the torque and can also reduce it. In the improved DTC, two vectors V3 and V6 are not used, and here there is an ambiguity in the flux vector [22]. In the improved DTC, the flux ripple value is less than the ripple value in the general DTC.

4. Direct torque control with 12 regions switching table method

In the general direct torque control (DTC), the two applied voltage vectors of V_i and V_{i+1} in the i -region created an ambiguity in torque and were practically useless. Thus, in the improved DTC with six regions, two applied voltage vectors of V_{i+2} and V_{i+5} created an ambiguity in increase or decrease of flux, and these two

vectors were not used. Now if the geometric location of the stator flux is divided into 12 regions, all applied voltage vectors in each region were usable and there was an ambiguity problem described in the methods, will be resolved. The geometric location of the stator flux with 12 regions is shown in figure 6. [1, 18]

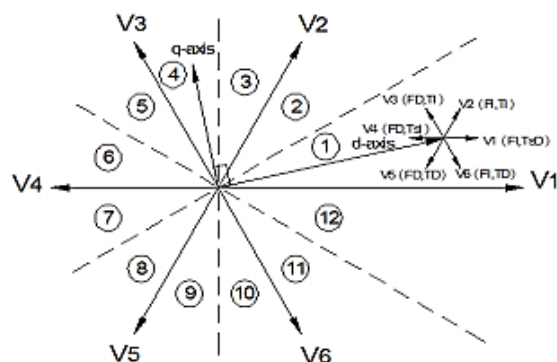


Fig.6. Voltage vectors and geometric location of stator flux with 12 regions[23].

- In figure 6:
- FI = Flux Increase
- FD = Flux Decrease
- TD = Torque Decrease
- TI = Torque Increase
- TSD = Torque Slight Decrease
- TSI = Torque Slight Increase

It should be noted that all voltage vectors are used in this method.

The 12 regions DTC switching table is listed in Table 4. It is clear that the voltage vector of V_1 will generate a relatively large increase in flux, as well as a slight decrease in torque in the 12th region. According to the switching table of 12-region method that given in table 4, hysteresis controller of torque has 4-levels and hysteresis controller of flux is 2-levels.

5. Simulation

To check the general direct torque control (DTC) performance and proposed methods for improved switching table and also, the 12-region switching table mentioned above, in the Matlab/Simulink, simulation of these methods are performed and simulation results are given below. In simulations, the hysteresis controller bandwidth of the torque is set to 0.5 and hysteresis controller bandwidth of the flux is set to 0.01.

In simulations, the dynamic model of Squirrel cage induction motor is used and the motor parameters used are as follows:

- $R_r = 1.34$ ohm
- $R_s = 1.77$ ohm
- $L_{lr} = 12.12$ mh
- $L_{ls} = 13.93$ mh
- $L_m = 369$ mh
- $P = 3$ kw
- $V_n = 380$ v
- Pole=4
- $j = 0.005$ kg.m²
- $B_m = 0.00001$

5.1. Electromagnetic Torque Curves

Electromagnetic torque curves for different switching tables are shown in figures 7-9. These curves are magnified and can be seen in figures 10-12. As you can see in the figures, the torque ripple in the general DTC switching table is better than the torque ripple in the improved switching table and also, the torque ripple in the 12-region switching table has a noticeable improvement over other switching table.

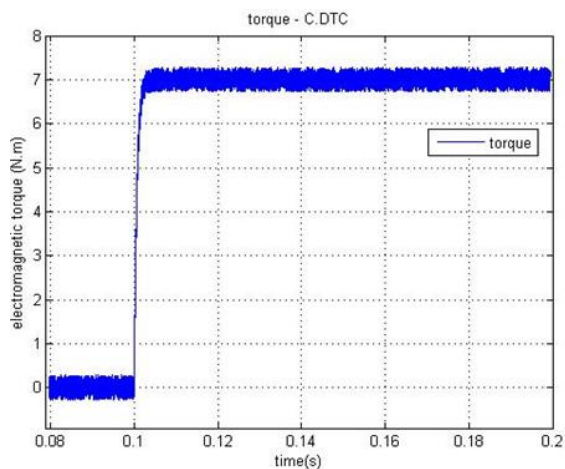


Fig.7. General DTC electromagnetic torque curve

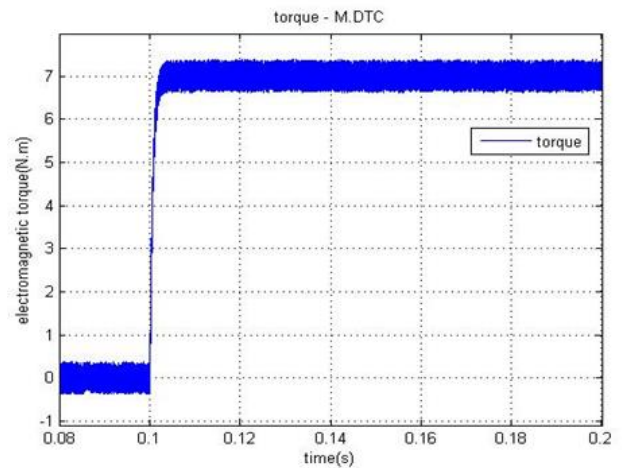


Fig.8. Improved switching table scheme torque curve

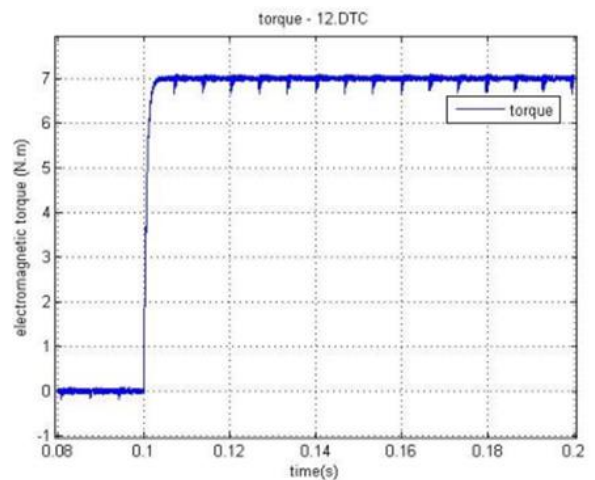


Fig.9. 12-region scheme torque curve

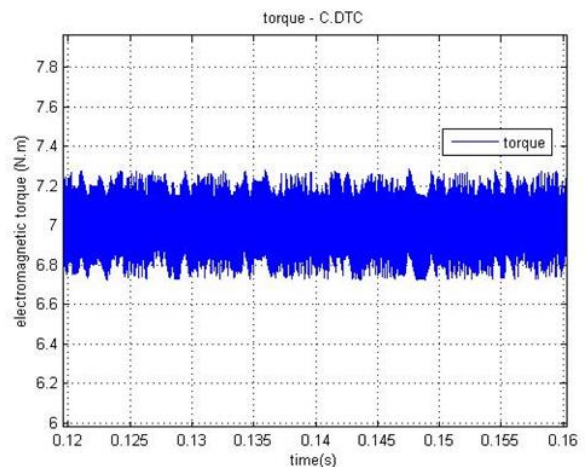


Fig.10. Magnified general DTC torque curve

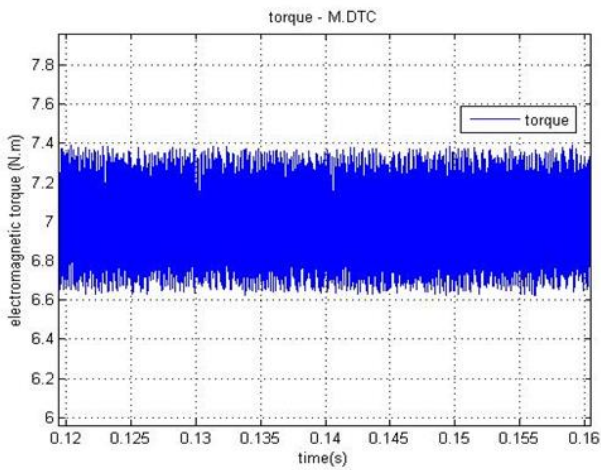


Fig.11. Magnified improved scheme torque curve

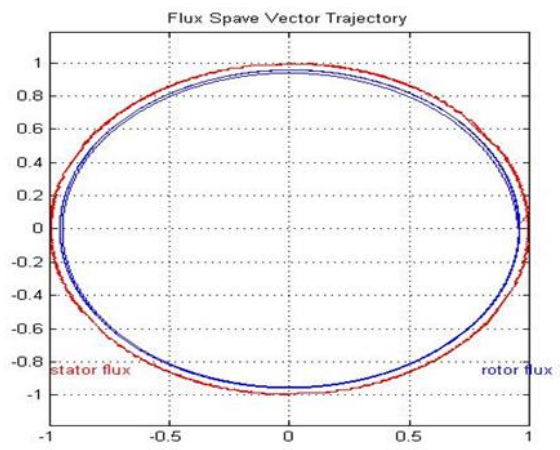


Fig.14. The geometric location of improved scheme stator flux

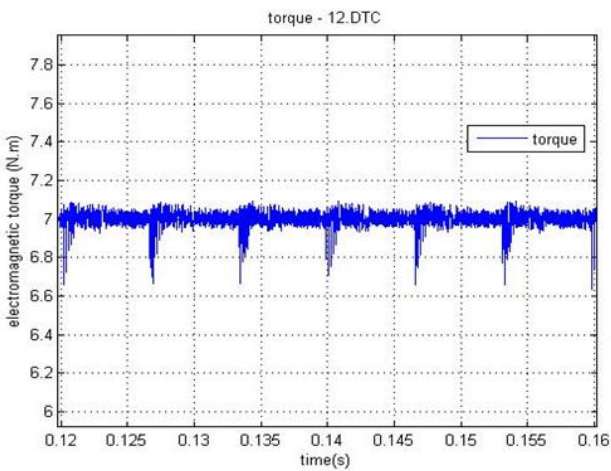


Fig.12. Magnified 12-region scheme torque curve

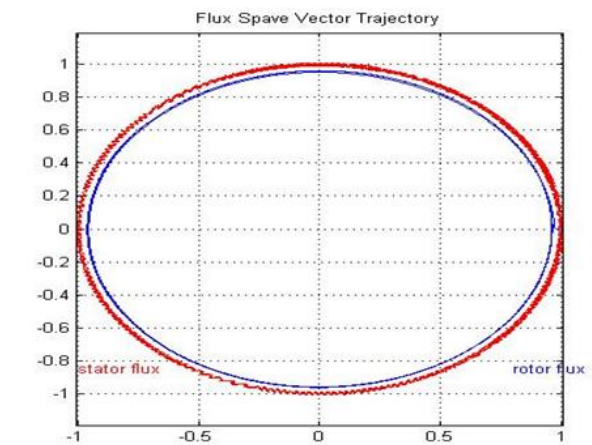


Fig.15. The geometric location of 12-regions scheme stator flux

5.2. Geometric Location Curves for Stator Flux

In figures 13-15, the stator flux curve is given in the general DTC, DTC with improved switching table and DTC with 12-regions switching table. According to the figures, it can be seen that the stator flux curve in the 12-regions method has improved relative to the general DTC method and this will reduce the harmonics of the stator current and improve its quality.

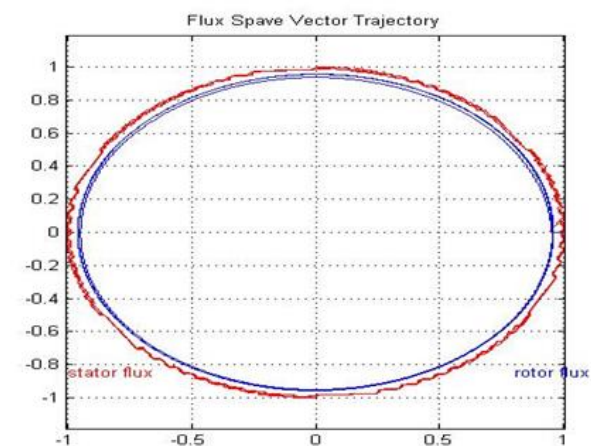


Fig.13. The geometric location of the general DTC stator flux

5.3. Rotor Speed Curves

Rotor speed curves are presented in figures 16-18 in triple methods of switching tables and its magnified curve in figures 19-21. Also, it should be noted that the load is applied to the system at the instant of 0.1 seconds and the speed decrease in the curves is also due to this issue.

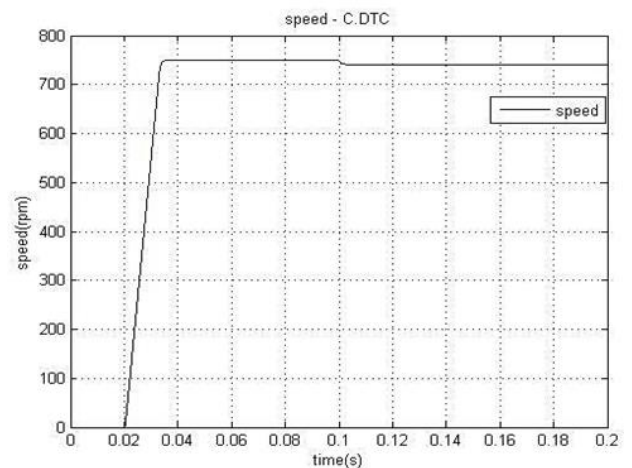


Fig.16. Rotor speed curve in general DTC

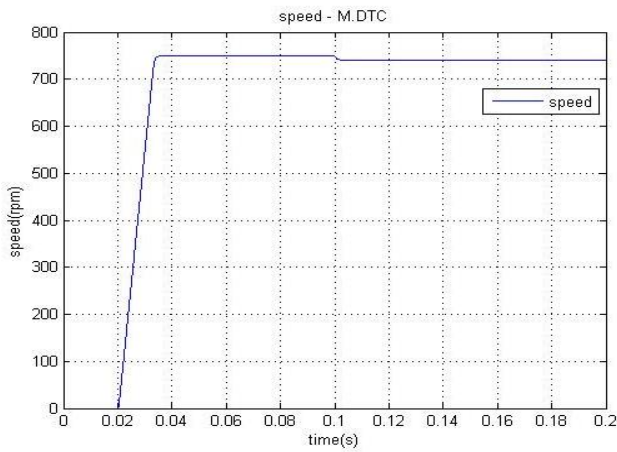


Fig.17. Rotor speed curve in improved scheme

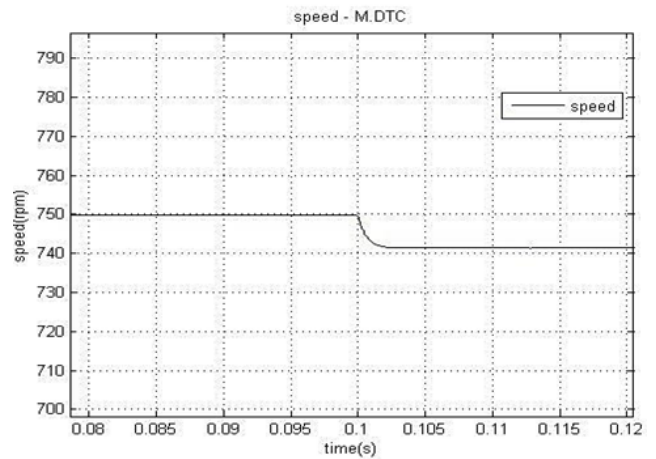


Fig.20. Magnified improved scheme speed curve

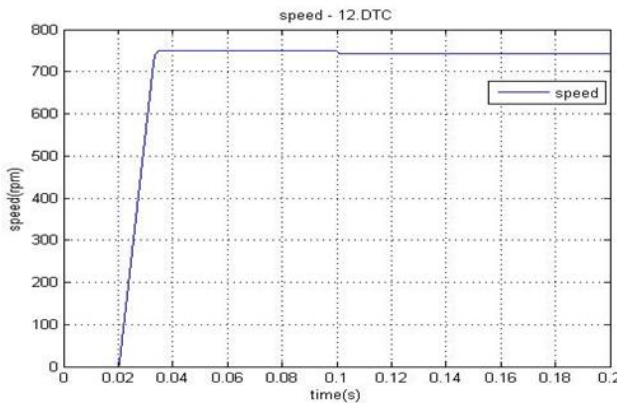


Fig.18. Rotor speed curve in 12-regions scheme

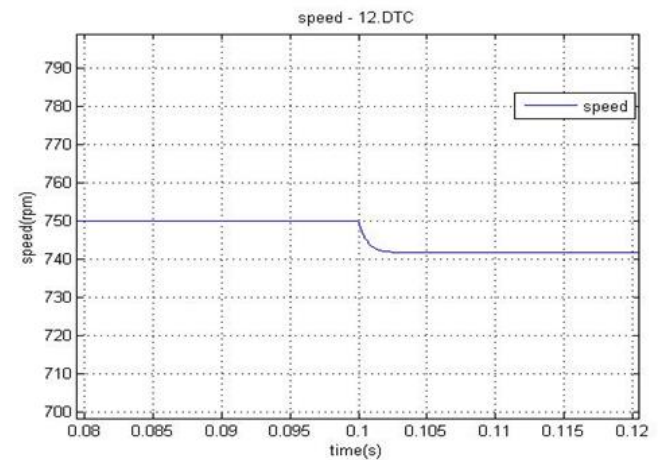


Fig.21. Magnified 12-regions scheme speed curve

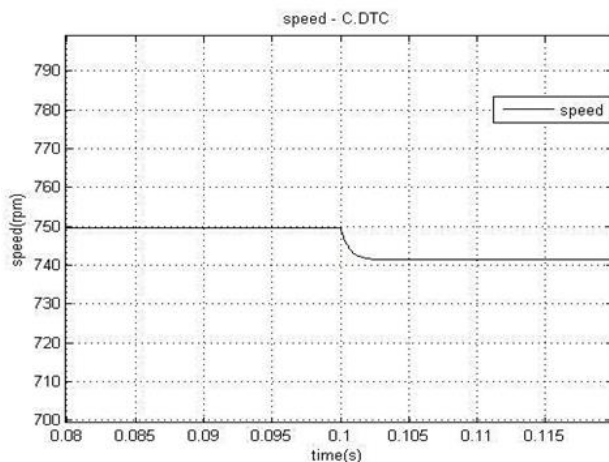


Fig.19. Magnified general DTC speed curve

6. Conclusion

In this paper, new switching tables for direct torque control were studied and compared and with the simulations of these new strategies, it was observed that in the direct torque control method with improved switching table and 6 regions decrease flux ripple but torque ripple will increase. But in direct torque control with the 12-region switching table, the flux and torque ripple decreases to an acceptable level. The dynamic response of the torque has acceptable speed in improved and general DTC technique and the 12 regions. Also, it was observed that the motor speed did not change significantly at the time of loading and almost it continues at about the same speed. It was found that the DTC method with 12-regions switching table has better performance than other tables and multi-levels inverters can be used to improve the performance of this strategy.

References

- [1] Bensaadi, Hacene, Youcef Harbouche, and Rachid Abdessmed. "Direct torque control (DTC-SVM) of PMSG based in wind energy conversion system." UPB Scientific Bulletin, Series C: Electrical Engineering and Computer Science 81.2 (2019): 227-240.
- [2] Z. Wu, G. Zhang, W. Du, J. Wang, F. Han, D. Qian, "Torque control of bolt tightening process through

adaptive-gain second-order sliding mode," *Measurement and Control*, vol. 53, no. 7-8, pp.1131-1143, Jul. 2020.

[3] K. Prathibanandhi, R. Ramesh, "Hybrid control technique for minimizing the torque ripple of brushless direct current motor," *Measurement and Control*, vol. 51, no. 7-8, pp. 321-335, Aug. 2018.

[4] Y. Cho, "Development and verification of individual motor control technology to improve the driving performance of independently rotating wheel type railway vehicle using hardware-in-the-loop (HIL) Simulator," *Measurement and Control*, vol. 54, no. 1-2, pp. 11-24, Dec. 2020.

[5] J. Tavoosi, "PMSM speed control based on intelligent sliding mode technique," *COMPEL - The international journal for computation and mathematics in electrical and electronic engineering*, vol. 39, no. 6, pp. 1315-1328, Sep. 2020.

[6] J. Tavoosi, M. Shirkhani, A. Abdali, A. Mohammadzadeh, M. Nazari, S. Mobayen, J.H. Asad, A. Bartoszewicz, "A New General Type-2 Fuzzy Predictive Scheme for PID Tuning," *applied sciences*, vol. 11, no. 21, Nov. 2021.

[7] Najib El Ouanjli, Saad Motahhir, Aziz Derouich, Abdelaziz ElGhizal, Ali Chebabhi, Mohammed Taoussi, "Improved DTC strategy of doubly fed induction motor using fuzzy logic controller," *Energy Reports*, vol. 5, pp. 271-279, Nov. 2019.

[8] El Ouanjli, N., Motahhir, S., Derouich, A., El Ghizal, A., Chebabhi, A., & Taoussi, M. (2019). Improved DTC strategy of doubly fed induction motor using fuzzy logic controller. *Energy Reports*, 5, 271-279.

[9] Baader, U., M. Depenbrock, G. Gierse, "Direct self control (DSC) of inverter-fed induction machine: A basis for speed control without speed measurement," *IEEE transactions on industry applications*, vol. 28, no. 3, pp. 581-588. May. 1992.

[10] M. Depenbrock, "Direct self-control (DSC) of inverter-fed induction machine," *IEEE transactions on power electronics*, vol. 3, no. 4, pp. 420-429. Oct. 1988.

[11] Casadei, D., G. Grandi, G. Serra, "Rotor flux oriented torque-control of induction machines based on stator flux vector control. in *Power Electronics and Applications*," Fifth European Conference on. Sep. 1993.

[12] Casadei, D., G. Grandi, G. Serra, "Study and implementation of a simplified and efficient digital vector controller for induction motors. in *Electrical Machines and Drives*,". 1993 Sixth International Conference on Electrical Machines and Drives (Conf. Publ. No. 376), Sep. 1993.

[13] D. Casadei, G. Grandi, G. Serra, A. Tani, "Effects of flux and torque hysteresis band amplitude in direct torque control of induction machines," *Proceedings of IECON'94 - 20th Annual Conference of IEEE Industrial Electronics*, Sep. 1994.

[14] M.R. Douiri, M. Cherkaoui, "Comparative study of various artificial intelligence approaches applied to direct torque control of induction motor drives," *Frontiers in Energy*, vol. 7, no. 4, pp. 456-467, Jul. 2013.

[15] A. Al-Quteimat, A. Roccaforte, U. Schäfer, "Performance improvement of direct torque control for doubly fed induction generator with 12 sector methodology," 2016 IEEE International Conference on

Renewable Energy Research and Applications (ICRERA), 2016, pp. 242-246.

[16] M. Essaadi, M. Khafallah, A. Saad, A. Hamdoun, H. Chaikhy, "A comparative analysis between conventionnal and new direct torque control strategies of induction machine," 2014 Second World Conference on Complex Systems (WCCS), 2014, pp. 350-354.

[17] T. S. Singh, A. K. Jain, "Improved Direct Torque Controlled IPM Synchronous Motor using variable band 12 sector control in two level inverter," 2016 IEEE 6th International Conference on Power Systems (ICPS), 2016, pp. 1-6.

[18] Vas, Peter., *Sensorless vector and direct torque control*. Oxford Univ. Press. 1998.

[19] M. Hafeez, M.N. Uddin, R.S. Rebeiro, "FLC based hysteresis band adaptation to optimize torque and stator flux ripples of a DTC based IM drive," 2010 IEEE Electrical Power & Energy Conference, Aug. 2010.

[20] M.P. Kazmierkowski, A.B. Kaspruwicz, "Improved direct torque and flux vector control of PWM inverter-fed induction motor drives," *IEEE Transactions on industrial electronics*, vol. 42, no. 4, pp. 344-350. Aug. 1995.

[21] A.M. Trzynadlowski, "The field orientation principle in control of induction motors," *Springer Science & Business Media*. 1993.

[22] Mokhtaril, B., et al., *Experimental DTC of an Induction Motor Applied to Optimize a Tracking System*. energy, vol. 12, 2012.

[23] E. Ahmed, A.R.A. Elwhab, S.A. Abo-Zaid, Elwany, "Torque Ripple Reduction in Direct Torque Control of Induction Motor Drives by Improvement of the Switching Table," *Journal of Multidisciplinary Engineering Science and Technology (JMEST)*, vol.1, no.5, pp. 238-243. Dec. 2014.